

Figure 1. Active Fiber Composite (AFC) actuators. Left: Architecture, mode of operation, and component materials. Right: Multiple AFCs produced in a production scale lamination press process.

Prior work on the theory, manufacturing, architecture, and the properties of AFCs has been described in detail elsewhere [1-4]. For reference, representative properties of a conventional AFC architecture are collected in Table 1.

Table 1. Representative Properties of Conventional AFCs.

PROPERTY	VALUE
Average Actuation Strain at 3 kV _{pp} under 600 V _{dc} bias (ppm)	1200 – 1400
Operational Voltage Limits (V)	-1500 to 2800
Elastic Compliances s_{33} (m ² /N)	40.0 X 10 ⁻¹²
s_{13} (m ² /N)	-11.0 X 10 ⁻¹²
s_{11} (m ² /N)	60.0 X 10 ⁻¹²
Piezoelectric Coeff. d_{33} (pm/V)	150
Relative Permittivity K_{33}	495
Density ρ (g/cm ³)	4.5

More demanding AFC applications require improved part-to-part consistency and greater mechanical displacement and force outputs. In the military sector, these applications include distributed integral actuators for active aeroelastic control in SensorCraft and unmanned combat air vehicles (UCAVs). In these applications, improvements in actuator strain and energy density are paramount. Other applications include structural-acoustic control on launch vehicle shrouds to reduce noise transmission to the payload, which require conformable actuators of high authority. At present, neither of these applications can be fully enabled with conventional AFC actuators. In many commercial applications, higher strain output at lower electric fields is needed to reduce costs associated with high voltage drive and control electronics.

To address the more demanding applications, we have implemented a new method to form free-standing piezofiber preform modules using a ceramic injection molding process. These preforms are easier to work with in actuator fabrication processes than loose fibers, and the shape of the fiber can be readily tailored by appropriate mold design. This allows for the incorporation of a higher volume fraction of piezoelectric material in the composite, and can be used to enhance electrical contact between fiber and electrode while reducing field-concentrating asperities and other fiber features associated with electric breakdown and other failure mechanisms. This paper describes: (1) the injection molding technology and its application to piezofiber modules for AFCs, (2) characterization of AFCs made with Type II PZT piezofiber modules, and (3) future directions to enhance AFC properties using both polycrystalline and textured polycrystalline PMN-PT piezofibers.

2. INJECTION MOLDING PROCESS FOR PIEZOFIBER MODULES

Injection molding (IM) technology for piezoceramics [5-7] has recently been adapted to produce high quality piezofiber preform modules for AFCs. Ceramics injection molding produces net shaped formed components with exceptional uniformity in both dimensions and microstructure. As a result, IM piezofiber modules produce very reproducible AFCs with consistently high performance. Piezoceramics injection molding begins by compounding PZT or PMN powder with a wax-based binder, and then granulating the compounded material as feedstock for injection molding. The ceramic-wax feedstock is processed using conventional injection molders, which heat the feedstock to the proper viscosity and then inject it rapidly under high pressure into a cooled mold. Because the heated feedstock flows as an incompressible liquid, the formed part has a very uniform green density and none of the voids or other internal defects which frequently occur in dry pressing or low pressure forming methods. The uniform green properties of IM piezoceramics result in corresponding uniform fired microstructures, dimensions, and electromechanical properties.

Geometric characteristics of the IM AFC preforms are shown schematically in Figure 2. The individual fibers have a rectangular cross section, on the order of 0.3 mm thick and 0.7 mm wide. This fiber cross-section enhances the electric field magnitude and uniformity within the fiber array. The fibers in the array are attached to a common cross strip on one end, allowing the entire array to be picked up and handled simply as a monolithic unit (Figure 3).

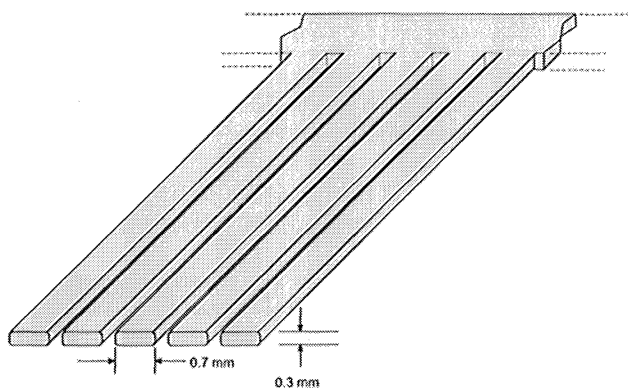


Figure 2. Configuration of injection molded piezofiber preform utilized in enhanced performance AFCs.

As discussed later in Section 4, the injection molding process for piezofiber preforms also facilitates even higher displacement AFCs powered by oriented PMN-PT fibers. Acicular seed crystals added to the IM feedstock are readily aligned as a result of the high shear forces naturally occurring during mold filling. The resulting solid state converted PMN-PT preforms and AFCs have the potential to provide at least twice the strain output.

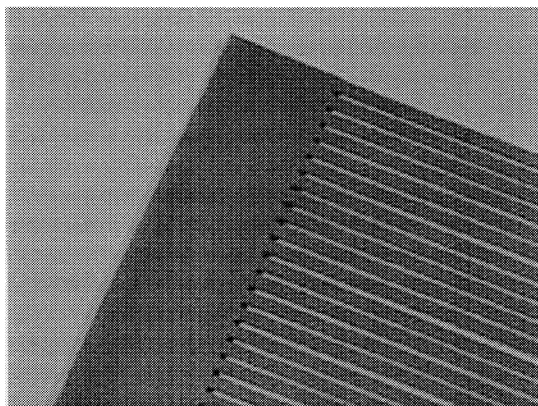


Figure 3. Photograph showing corner of connecting strip end of an injection molded PZT fiber preform.

3. CHARACTERIZATION OF INJECTION MOLDED PIEZOFIBERS IN PZT BASED AFCs

To evaluate the performance of injection molded fiber modules in the composite architecture, Type II PZT IM piezofibers were processed into standard 51 mm x 127 mm AFCs, as well as into AFCs of other geometries required for specific tests.

The following tests were carried out on these PZT AFCs:

- (1) Free strain measurements to determine strain-voltage behavior (population of 20 samples).
- (2) Resonance measurement to extract elastic modulus, piezoelectric and coupling coefficients at 25°C and 75°C (population of 4 samples).
- (3) Mechanical strain-stress tests to determine effective elastic moduli at 25°C and 75°C (population of 7 samples).
- (4) Electro-mechanical fatigue tests to determine temporal stability of AFC performance (population of 2 samples).

Brief summaries of the experimental procedures and characterization results for (1) - (4) are given below.

(1) Free strain measurements were conducted using 1 Hz AC fields at 0-26 kV/cm on 51 mm x 127 mm AFCs. Samples were poled at 120°C and 3 kV and aged before taking the measurements. The yield after poling was 85%. The average microstrain ($\mu\epsilon$) measured for the poled samples at the highest field applied (26.1 kV/cm) was $1830 \pm 30 \mu\epsilon$. The small variation of microstrain around the mean ($\pm 1.6\%$) demonstrates the excellent piezoelectric material quality and part-to-part uniformity achievable with this process in the standard AFC size and architectural configuration. A typical strain-voltage hysteresis loop is shown in Figure 4. The value of the low-field free piezoelectric coefficient, as determined by extrapolating the values obtained at intermediate field levels to zero, was $d_{33} = 195 \text{ pm/V}$, which compares favorably with the data given in Table 1 for AFCs made with the conventional loose-fiber process. At the highest voltage applied, the free piezoelectric coefficient was $d_{33} = 720 \text{ pm/V}$. However, piezoelectric coefficients determined in this way are not deterministic, as the shape of the microstrain-voltage loop may influence the absolute value of the results. In this respect, complementary measurements made using the resonant frequency technique are useful for comparison of low-field properties.

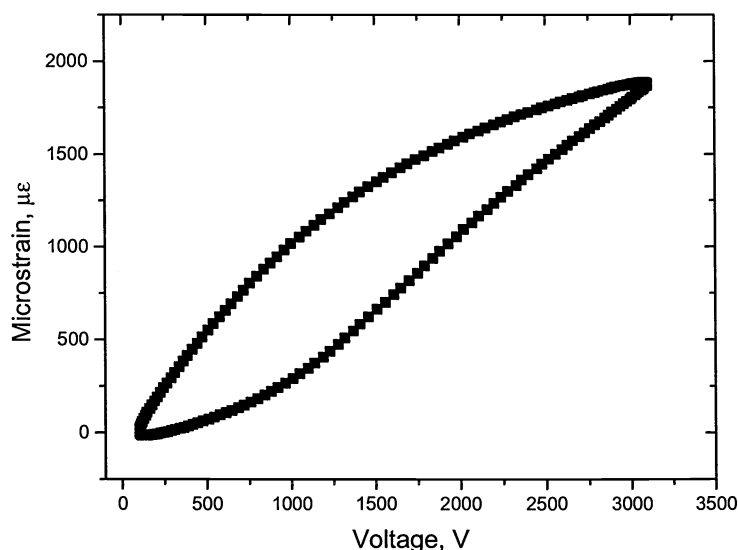


Figure 4. Electromechanical hysteresis loops measured for 51 mm x 127 mm AFCs manufactured from MSI injection molded fiber modules. Samples were poled at 120°C and at 3 kV. Measurements were taken at 1Hz. Electrode pitch is 1.14 mm (1 kV corresponds to 8.7 kV/cm). The low field and maximum field d_{33} coefficients are 195 and 720 pm/V, respectively.

(2) To gain more complete information on the elasto-dielectric properties of the composites, resonance measurements were carried out on 25 mm x 100 mm AFC test samples under a 3 kV bias at temperatures of 25 and 75°C. Table 2 summarizes the results of these tests, including piezoelectric coefficient (d_{33}), coupling factor (k), and elastic modulus (Y_{33}).

Table 2. Low-field Properties of AFCs made using IM PZT Piezofiber Modules.

Temperature (°C)	d_{33} (pm/V)	k (-)	Y_{33} (GPa)
25	133 ± 15	0.324 ± 0.063	23.2 ± 0.9
75	118 ± 26	0.320 ± 0.135	21.7 ± 1.1

From the table it is evident that although there is some variability in the measured elasto-dielectric parameters, both sets of measurements are in agreement with the historical low field values for loose-fiber AFCs of $d_{33} \sim 150$ pm/V, $k \sim 0.4$, and $Y_{33} \sim 20$ GPa. This variability observed here reflects ambiguities in the fine structure of the resonance peaks, leading to some subjectivity in the quantitative interpretation of the measurements. Within the limits of scatter, the two data sets collected at the 25°C and 75°C are not statistically different. As an additional confirmation of these numbers, the elastic properties were extracted directly from mechanical testing under load.

(3) Further measurements, to characterize mechanical behavior under load, were made under short circuit (constant electric field) boundary conditions. To conduct these tests, 25 mm x 132 mm AFC specimens were symmetrically laminated with 2 plies of 0°/90° E-Glass fabric and unidirectional strain gages and loading tabs were bonded on opposing sides of the specimen, as shown in Figure 5.

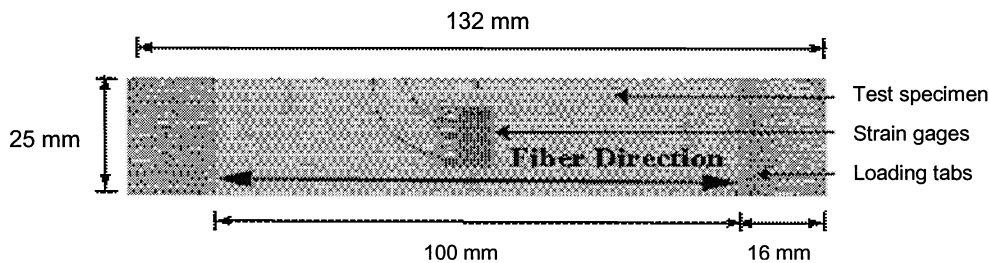


Figure 5. Test configuration for mechanical tests.

The test was carried out by placing the test rig in a controlled temperature enclosure maintained at either 25°C. The specimen was then placed in grips at either end at a 4.4 N nominal load, a value considered small compared to the maximum expected load of 980 N. The specimens were then loaded and unloaded to incrementally higher maximum strain levels, in the range of 500 to 6000 $\mu\epsilon$, in 500 $\mu\epsilon$ increments, at a rate of 5000 $\mu\epsilon/\text{min}$ (corresponding to 8.9 N/sec). The resulting strains and loads were continuously recorded at increments of ~ 5 $\mu\epsilon$ during loading and unloading, under load control mode of operation. Figure 6 shows the loading profile used.

Representative stress-strain curves for AFCs tested at 25°C are shown in Figure 7. A linear approximation connecting the terminus of each curve in Figure 7 to the origin was used to determine the effective elastic moduli along the fiber axis, as represented by the slope of each such line. The moduli so determined are plotted against the corresponding strain in Figure 8. Figure 8 shows the value of the AFC chord modulus extracted using standard laminated plate theory computations. At both temperatures, the chord modulus decreases rapidly at strain levels above about 3000 $\mu\epsilon$. However, even at strains as high as 2500 $\mu\epsilon$, the chord modulus retains useful values as high as 10 GPa at room temperature. As a cross check on the measurement technique, we note that the chord modulus determined in this way at room temperature is very close to that obtained from the resonant frequency measurements (~ 20 GPa). Measurements of the elastic moduli measured at an elevated temperature of 75°C, showed that the shapes of the curves were quite similar to the ones in Figure 8, and that the reduction in modulus at elevated temperature is nearly a constant 25-30% at all strain levels.

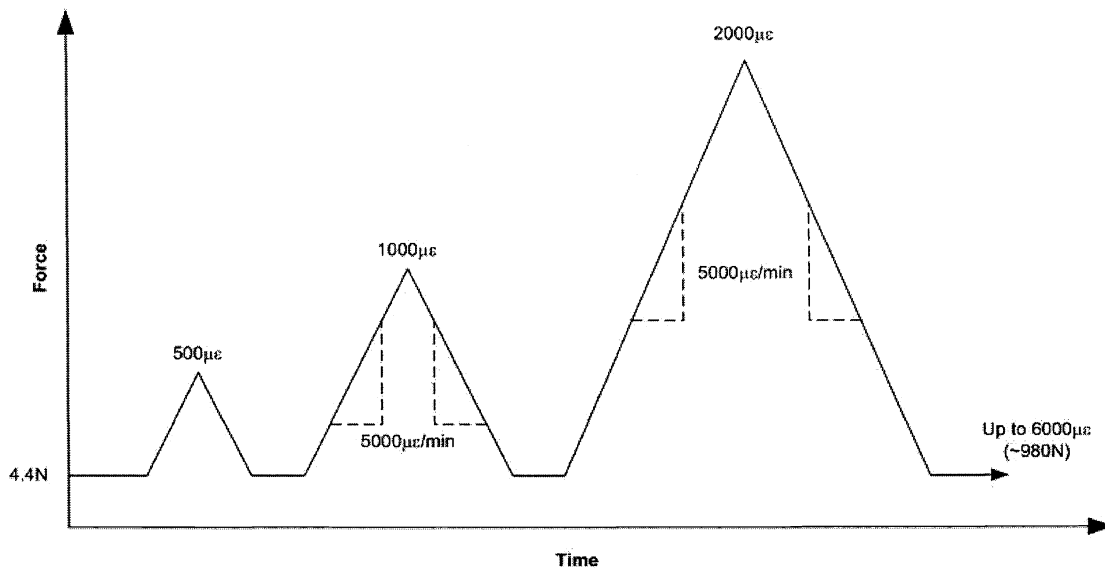


Figure 6. Load *versus* time profile used in stress-strain tests.

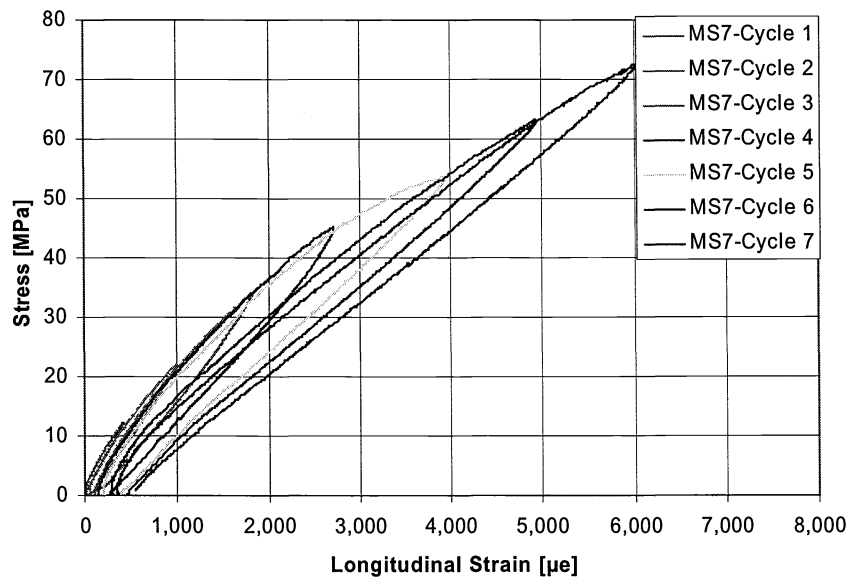


Figure 7. Typical stress-strain curves obtained at 25°C for AFCs fabricated from IM PZT piezofiber modules.

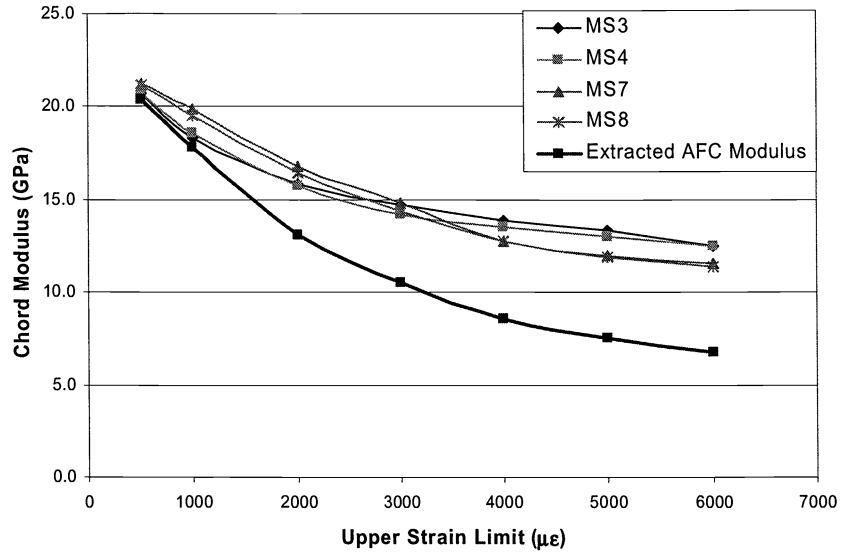


Figure 8. Chord modulus at 25°C for AFCs fabricated from IM PZT piezofiber modules. The AFC modulus is extracted using laminated plate theory computations.

(4) To assess the reliability of AFCs made with the injection molded piezofiber modules, electro-mechanical fatigue tests were performed on 51 mm x 127 mm AFCs at room temperature. Tests were conducted under a sinusoidal electric field at 100 Hz with an amplitude of 1 kV. Measurements of microstrain at intermediate numbers of cycles were taken at 8.7 kV/cm and 26.1 kV/cm at a measuring frequency of 10 Hz and a bias field of 600 V_{dc}. The measurement fields were chosen to represent fractions of the coercive field (E_c) corresponding to $E/E_c \sim 0.7$ and $E/E_c \sim 2.5$. As seen in Figure 9, there is no degradation in free strain out to ten million cycles at either test condition.

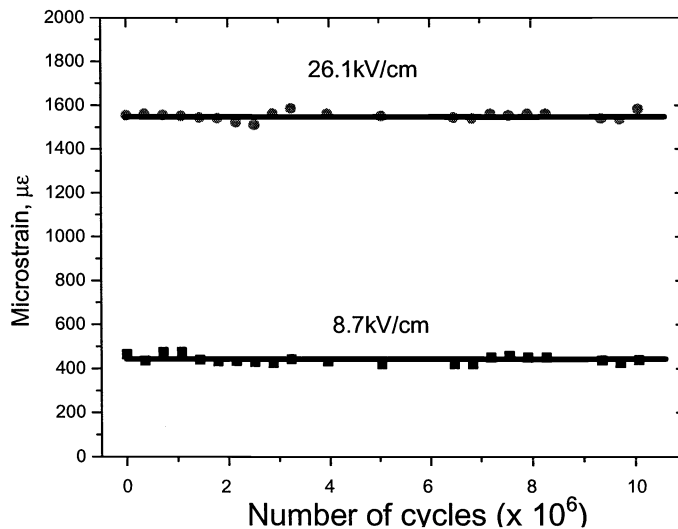


Figure 9. Results of electromechanical fatigue testing to 10 million cycles of AFCs made with IM PZT piezofiber modules at electric fields corresponding to $E/E_c \sim 0.7$ and $E/E_c \sim 2.5$.

4. FUTURE DIRECTIONS

The development of single-crystal piezoelectrics with exceptional electromechanical properties creates the possibility for dramatic increases in AFC actuation capabilities. An attractive route for the deployment of these materials in AFCs uses a solid-state conversion (SSC) approach to achieve texture by thermal treatment of fine matrix powders of $\text{Pb}(\text{Mg}_{1/3}\text{Nb}_{2/3})\text{O}_3\text{-PbTiO}_3$ (PMN-PT) containing properly oriented and aligned acicular seed crystals [8].

Predictions of the low-field piezoelectric properties made using the uniform field theory (UFM) [1] were used to estimate the performance enhancements attainable in polycrystalline PMN-PT and textured PMN-PT relative to conventional PZT piezoelectric materials. The results are shown in Figure 10. As seen in the figure, saturation values of d_{33} , corresponding to pure 33-mode actuation, range from $d_{33} \sim 200$ pm/V for PZT, to $d_{33} \sim 650$ pm/V for polycrystalline PMN-PT, to up to $d_{33} \sim 1000$ pm/V for single crystal materials.

The injection molding process provides an additional advantage in that the high shear forces generated during forming facilitate effective orientation of the acicular seed crystals necessary to promote grain growth. As a first step to developing these materials, we have performed preliminary tests on small (12.5 mm x 25 mm) AFC coupons made with polycrystalline PMN-PT piezofibers. The results of microstrain measurements on PMN-PT AFCs are presented in Figure 11. It is seen that the free strain characteristics are as expected for the PMN-PT piezoelectric composition, with reduced hysteresis, lower coercive field, and higher low-field strain response than the Type II PZT materials (see Figures 4 and 11). The zero-field piezoelectric coefficient, $d_{33} = 650$ pm/V, is more than three times greater than that of Type II PZT, and in very good agreement with the UFM predictions of Figure 10. At high voltages, where the strain saturates, the piezoelectric coefficients of PZT and PMN-PT AFCs are comparable, with $d_{33} = 760$ pm/V observed for the small coupons. Apparently, dielectric mismatch between fiber and polymer matrix does not limit performance, perhaps due to nearly ohmic contact of the rectangular fibers with the electrodes. When appropriate acicular seed crystals are introduced, injection molded SSC PMN-PT piezofibers will provide substantial additional performance enhancements to the next generation of active fiber composites.

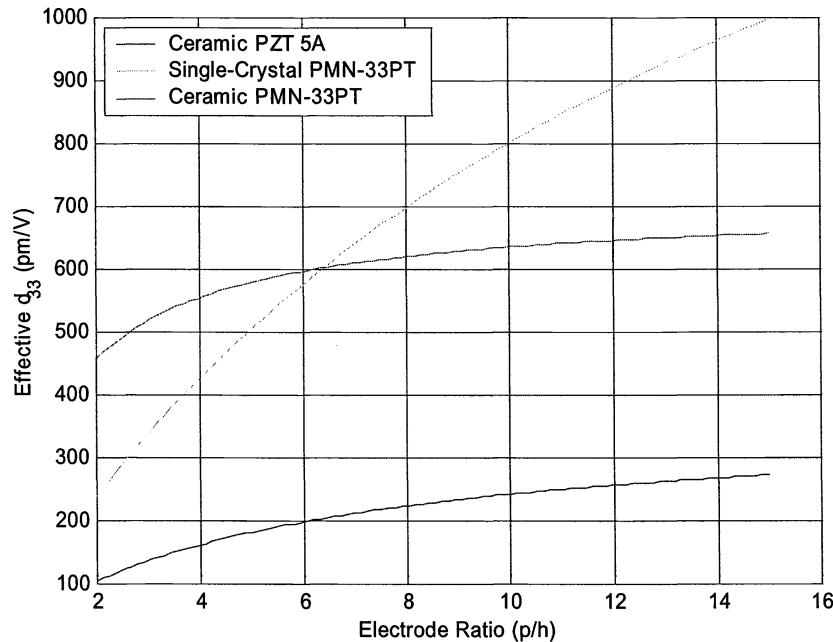


Figure 10. Free piezoelectric coefficients (d_{33}) against electrode pitch to fiber diameter ratio (p/h) for various piezoelectric fiber materials.

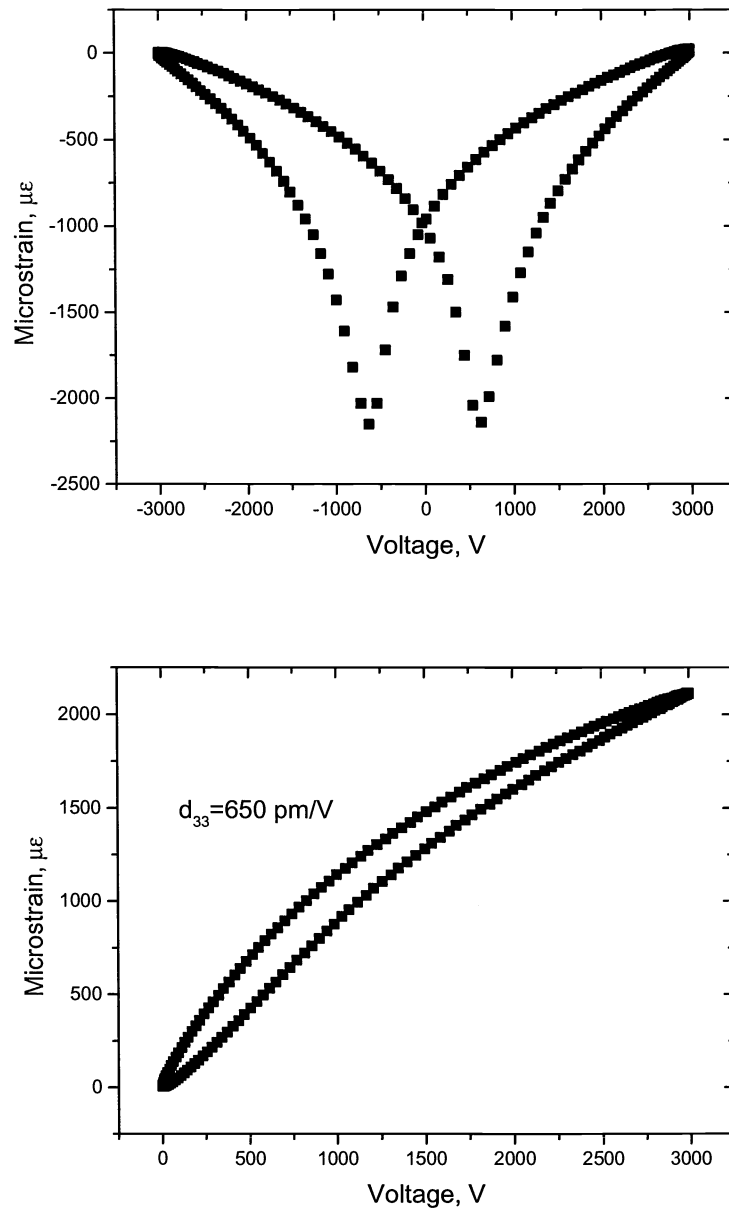


Figure 11. Electromechanical hysteresis loops measured for 12.5 mm x 25 mm AFCs manufactured from MSI PMN-PT piezofibers under bipolar (top) and unipolar (bottom) drive. Samples measured under unipolar drive were poled at 120°C and at 3 kV. Measurements were taken at 1 Hz. Electrode pitch is 1.14 mm (1 kV corresponds to 8.7 kV/cm).

5. CONCLUSIONS

This paper has presented a brief review of a unique combination of two complementary technologies: actuators in the form of active fiber composites, and injection molding to produce free standing piezofiber modules. Using electro-mechanical, resonant frequency, and mechanical tests, it has been shown that IM piezofiber preform modules produce AFCs that exceed the properties of those made with conventional loose-fiber processes. These preforms reduce part fabrication times, increase yields, and improve part-to-part consistency. In addition, further enhancements in AFC performance have been demonstrated using PMN-PT piezofiber modules. The AFC architecture, together with the high shear forces generated during injection molding, have distinct advantages for the exploitation of next generation piezoelectric materials based on highly textured polycrystalline ceramics that promise even larger strain response.

ACKNOWLEDGMENTS

This work was sponsored in part by DARPA/AFOSR and funded under AFOSR Cooperative Agreement Grant No. F49620-99-2-0332.

REFERENCES

1. A.A. Bent and N.W. Hagood, "Piezoelectric Fiber Composites with Interdigitated Electrodes," *Journal of Intelligent Material Systems and Structures* **8**, November 1997.
2. A.A. Bent, "Active Fiber Composite Material Systems for Structural Control Applications", SPIE Smart Structures & Materials, Newport Beach, CA, March 1999.
3. A.A. Bent and A.E. Pizzochero, "Recent Advances in Active Fiber Composites for Structural Control," SPIE Smart Structures & Materials, Newport Beach, CA, March 2000.
4. G.A. Rossetti, Jr., A.E. Pizzochero, and A.A. Bent, "Recent Advances in Active Fiber Composites Technology," *Proceedings of the 12th IEEE International Symposium on the Applications of Ferroelectrics (Vol. 2)* Honolulu, HI, July 2000.
5. R. Gentilman, D. Fiore, H. Pham, K. French, L. Bowen, "Fabrication and properties of 1-3 PZT-polymer composites," *Ceramic Transactions* **43**, pp. 239-247, 1994.
6. R. Gentilman et al., "1-3 piezocomposite smart panels for active surface control," *SPIE Proc.* **2721**, Feb. 1996, 234-9.
7. L. Bowen, R. Gentilman, H. Pham, D. Fiore, K. French, "Injection Molded Fine-Scale Piezoelectric Composite Transducers," *IEEE Ultrasonics Symposium* 1994, 499-503.
8. K. McNeal, R. Gentilman, C. Near, M. Harmer, H. Chan, A. Scotch, V. Venkatramani, C. Geskovich, "Processing and Application of Solid State Converted High-Strain Materials," SPIE's 7th International Symposium on Smart Structures and Materials 5-9 March 2001, Newport Beach, CA